Atmos. Chem. Phys. Discuss., 7, 12097–12143, 2007
www.atmos-chem-phys-discuss.net/7/12097/2007/

Atmospheric Chemistry and Physics Discussions

Ozone profile retrieval from limb scatter measurements in the HARTLEY bands: methodology, algorithm description, sensitivity studies, and validation

G. J. Rohen[1], C. v. Savigny[1], J. W. Kaiser[2], E. J. Llewellyn[3], L. Froidevaux[4], M. López-Puertas[5], T. Steck[6], M. Palm[1], H. Winkler[1], J. P. Burrows[1], M. Sinnhuber[1], and H. Bovensmann[1]

[1]Institute of Environmental Physics and Remote Sensing (IUP), Bremen, Germany
[2]European Centre for Medium-Range Weather Forecasts (ECMWF), Reading, UK
[3]Institute of Space and Atmospheric Studies (ISAS), Saskatoon, Canada
[4]Jet Propulsion Laboratory (JPL), Pasadena, USA
[5]Instituto de Astrofísica de Andalucía (CSIC), Granada, Spain
[6]Institut für Meteorologie und Klimaforschung (IMK), Karlsruhe-Leopoldshausen, Germany

Received: 2 July 2007 – Accepted: 4 August 2007 – Published: 16 August 2007

Correspondence to: G. J. Rohen (rohen@iup.physik.uni-bremen.de)

Abstract

SCIAMACHY limb scatter spectra have been used to retrieve atmospheric ozone profiles in the upper stratosphere and lower mesosphere. Through a selection of the wavelengths in the Hartley bands of ozone, profiles extending to 60 or 70 km altitude were retrieved. This constitutes the highest possible ozone profile information retrieval using the backscatter technique.

Comparisons with profiles measured by a ground based radiometer in Norway, MIPAS on board Envisat, HALOE on UARS and MLS on AURA indicate a good agreement of the ozone profiles in the upper stratosphere within 10 % but also an increasing overestimation above 50 to 55 km.

Sensitivity studies show that solar zenith uncertainty and tangent height errors are the largest error sources. Although the tangent height is corrected through an own retrieval the correction seemed to be be worser with increasing altitude and remains therefore as the largest error source for this presented profile retrieval.

1 Introduction

Retrievals of mesospheric ozone profiles from satellite limb scatter measurements using the backscatter technique have been done successfully for the first time from Solar Mesosphere Explorer (SME) spectra (Thomas et al., 1980; Rusch et al., 1983). An attempt to retrieve ozone in the Hartley bands from spectra measured by the Shuttle Ozone Limb Sounder Experiment (SOLSE) failed (McPeters et al., 2000) but introduced the retrieval approach using the so-called visible triplet instead. (Flittner et al., 2000).

Mesospheric ozone profiles are of special interest, e.g., for investigating of mesospheric properties or Sun-Earth interactions like solar proton events (Rohen et al., 2005) or solar cycle effects. The may also be required for the modeling of the atmospheric dynamics. At least, they help understand the atmospheric chemistry in the upper stratosphere and lower mesosphere.

ACPD

7, 12097–12143, 2007

This article presents results from mesospheric ozone profile retrievals from SCIAMACHY limb spectra using the backscatter absorption technique. A special attention is payed to the ozone content at highest possible altitudes by this special retrieval technique if wavelengths in the center of the Hartley bands are used. Also, disturbing emissions and stray light from outside the field of view of the spectrometer, as well as other error sources are discussed which may be a reason for the overestimation of the retrieved profiles above 50 km.

2 SCIAMACHY limb measurements

The Scanning Imaging Absorption spectroMeter for Atmospheric CHartographY (SCIAMACHY) (Bovensmann et al., 1999) is one of ten instruments on board ESA's Environmental satellite (Envisat). The satellite was launched in March 2002 into a sun-synchronous polar orbit at 799.8 km altitude with an inclination angle of 98.55°. This implies a fixed equator crossing time for the descending node; the local overflight times vary mostly around 10:00 a.m. during the day, depending on the latitude (see Fig. 1).

The SCIAMACHY spectrometer itself consists of eight channels between 214 and 2384 nm. The first channel - whose measurements are used for the presented profile retrieval - covers the lowest spectral region up to 314 nm with a spectral resolution of 0.21 nm.

Besides nadir (e.g., Buchwitz et al., 2005), solar occultation (Meyer et al., 2005), and lunar occultation measurements (Amekudzi et al., 2005), SCIAMACHY measures scattered light in the limb of the atmosphere from the surface to 95 km tangent height in steps of about 3.3 km (Schwab et al., 1996).

SCIAMACHY's instantaneous field of view in limb mode is 110×2.6 km (horizontal×vertical) at the tangent point. The horizontal *across* track coverage is 960 km with a resolution of 240 km at best. During a vertical scan within 60 s, Envisat moves 447 km; during the same time period, the tangent point moves due to the sphericity of the Earth in the opposite direction by about 145 km; both movements of

ACPD
7, 12097–12143, 2007

the tangent point result in an *along* track resolution of approximately 300 km.

Up to now, stratospheric ozone (up to 35 km) (von Savigny et al., 2003a), bromine oxide, nitrogen dioxide and chlorine dioxide (Rozanov et al., 2005) concentration profiles have been inferred successfully from SCIAMACHY limb scatter measurements.

3 Profile Retrieval Description

3.1 Methodology

The retrieval approach is based on the fitting of measured and modeled limb radiance profiles at discrete wavelengths, i.e., small spectral integration ranges of 2 nm. This technique was first proposed for air-borne limb measurements (e.g., Cunnold et al., 1973; Aruga and Heath, 1982) but was soon applied to SME satellite measurements (Rusch et al., 1983).

Although basically the maximum of ozone absorption cross sections in the Hartley bands (around 255 nm) appears more appropriate for ozone profile retrievals at higher altitudes (Wayne, 1987; Burrows et al., 1999; Bogumil et al., 2003), only wavelengths above 265 nm have been employed by now (Rusch et al., 1983), likely due to a low instrument signal. Higher accuracy is proposed if multiple wavelengths are used (Aruga and Heath, 1982).

A proper fit over a continuous wavelength range is difficult to obtain because emissions contribute to the measurements at large tangent heights.

No justification for the selection of wavelengths have been given for previous ozone profile retrievals. The inversion technique applied to SME measurements, up to now the solely successful ozone retrieval from satellite-borne limb backscatter measurements in the ultraviolet-B, exploits radiances at 265 and 296.4 nm (Rusch et al., 1983).

Ozone profile retrievals at wavelengths in the Hartley bands from SOLSE observations (McPeters et al., 2000) failed due to a bad signal-to-noise ratio, and even in the related theoretical elaboration (Flittner et al., 2000) no reasons for a selection of wave-

ACPD
7, 12097–12143, 2007

lengths at 300, 310, 322, 355, 525, 600, and 675 nm have been given. For their routine profile retrieval, radiances at eleven discrete wavelengths between 300 and 355 nm have been used (McPeters et al., 2000).

Contamination of the spectra by emission features may originate from atmospheric trace gases, or also from space debris entering the atmosphere (see, e.g., Carbary et al., 2003; Fritzenwallner and Kopp, 1998; Clemesha, 1995).

In the ultraviolet, the NO-γ emissions (see, e.g., Herzberg, 1950) impact considerably limb measurements at high altitudes (see Fig.2) because of the increasing NO concentration with altitude. Their contribution to the total limb radiances, e.g., at 80 km tangent height reaches 20 % at 255 nm; below 220 nm, these can be as strong as the ambient radiation (López-Puertas, 2000). The Vegard-Kaplan bands of N_2 ($X^1\Sigma_g^+ \leftarrow A^3\Sigma_u^+$) overlay the entire ultraviolet and visible spectral region but usually contribute less than 1 % to the ambient radiation. Several N_2 Second Positive (2P) emissions mainly above 295 nm are negligible (López-Puertas, 2000). Three atomic oxygen lines are also expected in the ultraviolet; two are caused by the ($^2P-^4S$) transition at 247.0 and 247.1 nm and another at 297.2 nm, originating from the ($^1S-^3P$) transition (Rees, 1989).

An averaged SCIAMACHY limb spectrum indicates emissions in the ultraviolet (Fig. 3). The NO-γ electronic transitions dominate the spectrum. Only emissions of magnesium at 280 nm can be identified, other metal emissions are not observable at the wavelength range of interest.

For this retrieval, thirteen wavelengths were selected at 250, 252, 254, 264, 267.5, 273, 283, 286, 288, 290.5, 305, 307, and 310 nm, avoiding emission lines while covering the full range in the Hartley bands. Slight adjustments have been done empirically before fixing the wavelengths.

Figure 4 displays the shape of limb radiance profiles in the ultraviolet. In an optically thin atmosphere, limb radiance increases with decreasing altitude due to enhanced scattering. At a certain tangent height, however, the atmosphere becomes optically thick due to absorption (e.g., ozone) and Rayleigh-scattering, and no additional pho-

ACPD
7, 12097–12143, 2007

tons from the outer line of sight reach the instrument. Below this "knee", radiance decreases or increases again depending on the ratio of Rayleigh scattering and ozone absorption.

In the first step of the inversion, the ultraviolet limb radiances I_{ik} (i denotes the index for wavelengths and k the index for tangent heights) are normalized with respect to the limb radiance $I_{ik_{\mathrm{ref}}}$ at a certain empirically chosen reference tangent height above the knee,

$$I_{ik}^{\mathrm{norm}} = \frac{I_{ik}}{I_{ik_{\mathrm{ref}}}}, \tag{1}$$

reducing multiplicative errors.

For a better convergence, the base 10 logarithm is used to compose a retrieval vector 5 of 13 wavelengths×21 tangent heights=273 elements. For better convergence the base 10 logarithm is used.

The inversion of the measurement vector is performed by a nonlinear *Optimal Estimation* iteration scheme (Rodgers, 1976),

$$\boldsymbol{x}_{n+1} = \boldsymbol{x}_0 + \mathbf{S}_{\mathbf{x}_0}\mathbf{K}_{\mathbf{n}}^{\mathbf{T}}\left(\mathbf{K}_{\mathbf{n}}\mathbf{S}_{\mathbf{x}_0}\mathbf{K}_{\mathbf{n}}^{\mathbf{T}} + \mathbf{S}_{\mathbf{y}}\right)^{-1} \times \left((\boldsymbol{y} - \boldsymbol{y}_n) - \mathbf{K}_{\mathbf{n}}\left(\boldsymbol{x}_0 - \boldsymbol{x}_n\right)\right), \tag{2}$$

where $\boldsymbol{x}_{n+1}$ corresponds to the logarithm of the ozone profile estimate after $n+1$ iterations. $\boldsymbol{x}_0$ denotes the logarithm of the a priori profile which is provided by the five-year United Kingdom Universities Global Atmospheric Modeling Programme (UGAMP) climatology (Li and Shine, 1995) based on SME, Solar Backscatter UltraViolet (SBUV) (Fleig et al., 1990), Stratospheric Aerosol and Gas Experiment (SAGE II) (McCormick et al., 1989), and on ozone sonde measurements. $\boldsymbol{y}$ denotes the measurement vector. $\boldsymbol{y}_n$ is the modeled measurement after n iteration steps.

$\mathbf{K}$ in Eq. 2 denotes the respective weighting function matrix and $\mathbf{S}_{\mathbf{x}_0}$ the a priori covariance matrix. The off-diagonal elements of the covariance matrix are the covariances

with respect to the elements $x_{a,i}$ and $x_{a,j}$ taken from the climatology. The following a priori covariance matrix was used,

$$(\mathbf{S}_{\mathbf{x}_0})_{ij} = (\sigma_{x_0})^2_{ii} \exp\left(-\frac{z(i) - z(j)}{h}\right). \quad (3)$$

$(\sigma_{x_0})_{ii}$ is the standard deviation of the climatology and is set to 0.65, $z(i)$ and $z(j)$ are the corresponding altitudes, the length scale h is set to 3.3 km. The measurement variance matrix $\mathbf{S_y}$ is set to a standard deviation of 0.1.

The iterative inversion is truncated if

$$\chi^2 = \chi^2_x + \chi^2_y, \quad (4)$$

(see Rodgers, 1976) is below a predefined value which is found empirically. Here, the summands are

$$\chi^2_x = (x_0 - x_n)^T \mathbf{S}_{\mathbf{x}_0} (x_0 - x_n) \quad (5)$$

and

$$\chi^2_y = (y - y_n)^T \mathbf{S_y} (y - y_n). \quad (6)$$

The radiative transfer model SCIARAYS (Kaiser and Burrows, 2003) derives single Rayleigh and aerosol scattering, refractive bending and trace gas absorption in a fully spherical geometry. Aerosol absorption, clouds, and thermal emissions are not considered. GOME FM ozone cross sections (Burrows et al., 1999) are used for the derivation of the ozone absorption. Weighting functions are derived analytically.

Air densities and temperatures are provided by a monthly resoluted climatology derived by a chemical transport model, employing pressure and temperatures (Nagatani and Rosenfield, 1993) and ozone columns (McPeters, 1993) from a compilation of several models and measurements (McLinden et al., 2000). The spatial resolution of this climatology is 5° both in longitude and latitude.

Although SCIARAYS derives also Rayleigh scattering up to second order, only first order of scattering is used for this inversion since ozone in the Hartley bands absorbs

massively and allows almost no multiple scattering. SCIARAYS derives a solution of the radiative transfer equation, in integral form, i.e., radiances on each path through the atmosphere are integrated. The relative contributions of the respective paths as modeled by SCIARAYS are depicted in Fig. 5, demonstrating the dominance of single scattering in the spectral region of interest in this work.

The retrieval methodology provides sensitivity to ozone between about 30 and 60 km, sometimes 65 km (see first results Rohen et al., 2005). Weighting functions (Fig. 6) indicate a continuous coverage at all altitudes.

Figure 7 shows that fits and residuals for all thirteen wavelengths. Averaged residuals between 35 and 65 km are below 3 % (Rohen et al., 2005).

4 Sensitivity studies

4.1 Pointing errors

The accuracy of the tangent height registration can be improved by different techniques, e.g., using the shape of the radiance profiles (Janz et al., 1996; McPeters et al., 2000; Sioris et al., 2003; von Savigny et al., 2003b), or using CO_2 emissions (von Clarmann et al., 2003). For this presented retrieval, Tangent height Retrieval by Ultraviolet-B Exploitation (TRUE) VERSION 1.4 (Kaiser et al., 2004; von Savigny et al., 2005a) was employed which applies the former technique. TRUE is supposed to improve the accuracy to 500 m (von Savigny et al., 2005a).

An example indicates the errors caused by incorrect tangent heights for a sample profile retrieval (Fig. 8); an error of 2.5 km results in 90 % difference in ozone, and a shift of the radiance profile by 0.5 km leads to an error of up to 17 %. Error increases with altitude due to decreasing ozone scale heights.

ACPD
7, 12097–12143, 2007

4.2 Accuracy of solar zenith angle registration

The retrieval is sensitive to the solar zenith angle, in particular at large solar zenith angles whereas the solar azimuth angle has almost no impact on the retrieval (von Savigny, 2002).

Angles are registered for the left and for the right side, and for the center of the field of view; the latter is taken for the retrieval. Both the movement of the satellite and the averaging along the swath of 960 km can cause an angle inaccuracy of up to 2°.

The effect of this inaccuracy is shown in Fig. 9, for a small and a large solar zenith angle, respectively. Induced errors reach 13 % whereas almost no impact is observable at small solar zenith angles.

4.3 Stray light

External stray light is referred to as the contamination from outside the field of view, e.g., from cities or clouds. Stray light increases strongly where the signal-to-noise ratio is low, e.g., at high altitudes.

External stray light has been investigated, e.g., for the Optical Spectrograph and InfraRed Imaging System (OSIRIS) (Llewellyn et al., 2004); at 400 nm, it reaches 65 % at 70 km tangent height, and even 440 % at larger wavelengths and higher altitudes (Llewellyn and Gattinger, 1998).

The SCIAMACHY stray light exhibits approximately the same magnitude as those of OSIRIS (van Soest, 2005). By subtracting the background signal, channel 1 of SCIAMACHY was found to be not as strongly affected as the channel 2 whose contaminations at high tangent heights can be five to ten times larger than the ambient radiation.

In our sensitivity study, SCIAMACHY stray light was estimated at 310 nm by subtraction of the modeled from the measured radiances. Radiances smaller than 310 nm are less affected (van Soest, 2005), see also Fig. 7. The impact on a sample retrieval is shown in Fig. 10.

ACPD
7, 12097–12143, 2007

EGU

Stray light at 76 km reaches 120 % of the in-field signal whereas the impact on the profile retrieval is small. Induced errors never exceed 1 % between 35 and 65 km; in summary, stray light has a large impact on the measurements only above around 70 km, and hence has almost no effect on the retrieval in the region of interest between 30 and 60 km. This shows that the overstimation of the SCIAMACHY profiles cannot be reasoned only by this error source.

4.4 Scattering modes

The small impact of multiple scatter events in the Hartley bands has been demonstrated by model studies (Oikarinen et al., 1999; Loughman et al., 2005). Oikarinen et al. (1999) derived the single scattering contribution below 300 nm to be larger than 99 %.

Figure 5 shows the fraction of double scattered radiation in the atmosphere as derived by SCIARAYS. At 60 km, this fraction is about 5 % at 310 nm and decreases to 1 % below 290 nm.

Figure 11 now shows the impact of double scattered photons on the retrieval. Maximum multiple scattering is expected for SCIAMACHY measurements at about 35° solar zenith angle, which is approximately the minimum solar zenith angle along SCIAMACHY orbits. Omitting twice scattered photons causes retrieval errors below 3 %, even at 33 km. Thus, in order to save computing time, only single scattering is considered for the retrieval.

4.5 Aerosols

Due to sporadic aerosols entries, e.g., by meteorites (Hunten et al., 1980), rocket exhausts (Fricke et al., 1995), the amount of mesospheric aerosols is small, variable and difficult to quantify.

Noctilucent clouds (Gadsden and Schröder, 1989; Kokhanovsky, 2005; von Savigny et al., 2005c) affect the majority of limb measurements at polar latitudes in the summer hemisphere (von Savigny et al., 2005c). Those affected measurements are therefore

not usable for retrievals. An upstream cloud detector was implemented to reject measurements with noctilucent clouds signatures.

The negligible impact of aerosols in the upper stratosphere has already been shown for OSIRIS as well as for SCIAMACHY (von Savigny, 2002; von Savigny et al., 2005b). Thus, aerosols are not considered for the retrieval.

4.6 Ground albedo

The contribution of reflected photons to SCIAMACHY limb radiance measurements below 310 nm is less than 1 % due to massive ozone absorption (Fig. 5). Ground albedo is therefore also expected to have a negligible impact on the retrieval of profiles above 35 km.

Figure 12 shows the induced errors due to omitting surface reflection in the case of a SCIAMACHY measurement at a relatively small solar zenith angle. The contribution of reflected photons at 50 km tangent height is almost zero and increases to 2.2 % at 33 km which agrees with findings for stratospheric ozone profile retrievals with maximum errors between 3.5 and 5 % (55° solar zenith angle, 40 km altitude von Savigny, 2002).

4.7 A priori information

Presentations of the averaging kernels show the independence of the retrieval on a priori information (Fig. 3 of Rohen et al., 2006) for altitudes between 35 and 60 km. Retrieved ozone profiles using different a priori information (50 % difference) exhibit up to 4 % differences (Fig. 13).

At the edge of the retrieval sensitive altitude range, the a priori affects also the effects of the other error sources on the retrieval; the a priori may amplify or lower the effect of the error source depending on the relative position of the a priori and the ozone guess from the fitting. Since the sensitivity studies are based on different a priori profiles from the climatology this may reason why errors are sometimes higher or lower than found

ACPD
7, 12097–12143, 2007

through the sensitivity studies. We will use this later as one explanation for the high differences at the profile comparisons.

4.8 Temperature dependence of ozone cross sections, in the derivation of density, background density

Tabulated Global Ozone Monitoring Experiment (GOME) flight model (FM) ozone absorption cross sections (Burrows et al., 1999) are interpolated for usage in the retrieval, available at five temperatures differing by 20 K.

Figure 14 shows the errors induced by applying improper cross sections at 273 K and 293 K.

At lower altitudes, i.e., where ozone absorbs in the Huggins bands, errors of up to 4 % are induced. Absorption at higher altitudes (i.e., in the Hartley bands) is almost independent on temperature.

The temperature also determines the air density through the ideal gas law. The effect caused by lowering the air density by 5 % (which is a rough estimate) is depicted in Fig. 15.

Table 1 gives an overview of the sensitivity studies.

5 Validation

The validation presents comparisons with ozone profiles from MIPAS on Envisat, the Radiometer for Atmospheric Measurements (RAM) in Spitsbergen, the HALogen Occultation Experiment (HALOE) on the Upper Atmospheric Research Satellite (UARS) and the Microwave Limb Sounder (MLS) on AURA. SCIAMACHY (L0-L1) processor VERSION 5.4 and TRUE VERSION 1.4 have been used.

Figure 16 shows the overall statistics for all instruments which are discussed in the next sections.

The mean difference is below 10 or 20 %, depending on the altitude, with mean 1σ

ACPD
7, 12097–12143, 2007

deviation of below 20 %. Comparisons with MLS and MIPAS profiles show an overestimation above 55 or 50 km.

It should be noted at this place that also observations of ozone depletion during the Halloween solar storm – using profiles from the presented profile retrieval – agree fairly well with observations of e.g., Global Ozone Monitoring by Occultation of Stars (GOMOS), or the Solar Backscatter Ultraviolet Instrument (SBUV II) (Rohen et al., 2005). Those comparisons may also help to state the quality of the retrieval, even for measurements made under extreme conditions like a during a solar storm.

We will discuss the comparisons as shown in Fig. 16 in more detail, beginning with MIPAS.

5.1 Comparisons with MIPAS (IMK) ozone profiles

Used MIPAS ozone profiles were retrieved at the Institut für Meteorologie und Klimaforschung (IMK) (von Clarmann et al., 2001, 2003; Glatthor et al., 2005; Glatthor et al., 2006, and references therein) and provide a vertical coverage from 6 km to 68 km. MIPAS's field of view is 30 km horizontally and 3 km vertically.

MIPAS and POAM III (Lumpe et al., 2003) ozone profiles between 10 km and 60 km show agreement within 10 %, as well as comparisons with several LIDAR and ozone sonde measurements, and with ozone profiles from HALOE (Steck et al., 2007). MIPAS profiles have also been compared to SCIAMACHY stratospheric ozone observations and those of Global Ozone Monitoring by Occultation of Stars (GOMOS) (Bracher et al., 2005). In terms of GOMOS, the agreement of the compared profiles is also within 10 % up to 60 km altitude.

For comparisons, collocated measurements must have been performed at the same solar zenith angle, the maximum difference of the solar zenith angle is set to less than 2°. The number of coincident SCIAMACHY and MIPAS profiles is large due to the fact that both instruments are on Envisat. Thus, the spatial radius of coincident observations can be chosen small, 100 km or 200 km.

The general agreement is fairly good, but increasing differences with altitude are

ACPD
7, 12097–12143, 2007

observable which are enlarged above about 50 km. The increasing differences with altitude are due to the increasing ozone scale height. The reason for the increased differences above 50 km may be due to the fact that the TRUE retrieval uses ozone climatologies below 50 km what may result in an more inaccurate tangent height retrieval above this altitude. Solar zenith angle as a possible reason is most likely excluded since this error sources affect all altitudes in the same extent. The same is valid for the a priori error source. Stray light was shown to have not such strong effects on the retrieval (see the sensitivity studies).

5.1.1 Possible latitudinal and solar zenith angle dependence

Comparisons with MIPAS profiles in the polar and mid latitude region including the tropics are shown in Fig. 17 which indicate only a slight but characteristic dependence of the profile retrieval on the latitude. The already mentioned overestimation above 50 km can be seen for all latitude bands. Increasing differences at 45 to 50 km - possibly caused by a wavelength gap around 300 nm in the retrieval - can also be seen, but only as a weak feature at midlatitude bands. In contrast to that, the increasing differences due to the tangent height misregistration is clearly observable at midlatitudes but not that clear at the polar regions. This may also be related to the fact that the TRUE tangent height retrieval uses only tropical ozone climatologies.

Almost the same features like in Fig. 17 can be seen at the comparisons for different solar zenith angles (Fig. 18). Again, a clear overestimation between 50 and 60 km altitude can be observed in all figures, but the previously described feature at 45 km appears only at solar zenith angles below 60°, what shows that this feature is not caused by the methodology solely. It should be noted as this place that only measurements at solar zenith angle below 83° are used for the profile retrieval. Thus, Fig. 18 has no expressiveness for solar zenith angles above this number of degree. Anyway, the retrieval is almost not affected by the position of the Sun, although, again, the main already described increasing differences with altitude remain.

ACPD
7, 12097–12143, 2007

5.2 Comparison with HALOE ozone profiles

Next, comparisons with profiles from the HALOE instrument will be shown. The current HALOE UARS (Russell et al., 1993) ozone retrieval VERSION 1.9 provides profiles up to 70 km. Comparisons have been done with numerous instruments, including ozone sondes, LIDARS, balloons, rocketsondes, and satellites (Brühl et al., 1996; Rusch et al., 1997). HALOE profiles up to 50 km are in good agreement with SAGE II measurements. Above 50 km, HALOE observations are supposed to overestimate ozone by up to 20 % due to incorrect photochemical factors (Natarajan et al., 2005; Nazarayan et al., 2005), but this needs to be confirmed by more statistical analysis in the future, since only samples have been taken in order to show the improvements.

5.2.1 Photochemical modeling of solar occultation observations

Solar occultation measurements like made by HALOE are performed at local times which are characterized by minimum ozone concentrations (see Fig. 19).

In order to compare those HALOE solar occultation observations with SCIAMACHY limb observations, collocated HALOE measurements have been modeled photochemically, using a one dimensional version of the Single Layer Isentropic Model of Chemistry And Transport (SLIMCAT) model (Chipperfield, 1999) (Fig. 20).

For instance, differences between ozone at 90° and 74° solar zenith angle are of up to 20 % below 60 km and up to several hundred percent above 60 km. The detailed model errors and a summary of uncertainties for SCIAMACHY and HALOE ozone profiles are shown in Rohen (2006) and will therefore not be shown a second time.

The mean differences between the compared profiles indicate a fairly good agreement in terms of the statistical mean (Fig. 16). But the modeled HALOE ozone profiles provide large errors and make it therefore almost impossible to give a reliable statement about the quality of the profiles, at least above 50 km. Below 50 km, the agreement is fairly good, like at the comparisons with MIPAS profiles. However, this may confirm at least the good quality of the retrieved profiles below 50 km.

ACPD
7, 12097–12143, 2007

5.3 Comparisons with ground based radiometer measurement

Comparisons were also done with ground based measurements from the Radiometer for Atmospheric Measurements (RAM) over Ny Ålesund (78° N, 11° E), Norway (Langer, 1999).

RAM is a millimeter-wave radiometer tuned to the frequency of an ozone transition line at 142 GHz. Retrieved ozone profiles cover 15 to 55 km and exhibit a vertical resolution between 8 km and 20 km (Palm et al., 2005).

RAM profiles are validated by ozone sondes between 18 km and 24 km within 10 %, and with LIDAR instruments between 16 km and 34 km within 11 % (Palm et al., 2005). MLS observations have been used for validation between 20 and 55 km which also show an agreement within 10 % (Langer, 1999).

In order to compare SCIAMACHY and RAM ozone, SCIAMACHY ozone profiles were convolved by the averaging kernels of the RAM ozone retrieval. In spite of the poor vertical resolution, collocated ozone profiles indicate an agreement within 10 % (Fig. 16). Only a slight overestimation is observable above 50 km, but this smaller differences above 50 km - as seen in the MIPAS comparisons - may be due to the poor vertical resolution of the RAM profiles. Again, a reliable statement of the quality of the retrieved profiles above 50 km through this comparison is difficult to give.

5.4 Comparisons with MLS AURA measurements

Profiles as retrieved from MLS AURA may clear the quality of the retrieved profiles at higher latitudes at last.

Two years after launch, the first early validation analyses of VERSION 1.5 MLS on AURA ozone profiles have been published (Froidevaux et al., 2006). Validation has been done up to altitudes of 0.1 mbar (about 48 km) with ozone profiles measured by HALOE, Stratospheric Aerosol and Gas Experiment II (SAGE II), POAM III, and Advanced Composition Explorer (ACE). The MLS ozone profiles agree well within 5 % with the compared profiles in the lower stratosphere, but also an underestimation in

the upper stratosphere and an overestimation towards the mesosphere is observable. Although an upper limit of 0.46 mbar (about 54 km altitude) was recommended for the ozone product, good sensitivity in the upper mesosphere is also proposed (Livesey et al., 2005).

A statistics from collocated SCIAMACHY and MLS profiles within 300 km radius (Fig. 16, right, bottom) shows a remarkable good agreement up to 55 km, but again an overestimation of the SCIAMACHY profiles above that height. But, in contrast to the MIPAS comparisons, deviations become considerable only above approximately 56 km, 5 km lower than in the case of MIPAS, and the effects of the tangent height misalignment is less stronger. The increased differences at 45 km are also indicated.

6 Conclusions

We used SCIAMACHY/Envisat limb scatter measurements in the Hartley bands of ozone to retrieve ozone profiles in the upper stratosphere and lower mesosphere between approximately 35 and 65 km, with a special attention to prove whether this methodology is capable to retrieve information about the content at higher altitudes up to 70 km. At least, sensitivity at higher altitudes (up to 70 km) was reached at large solar zenith angles, but in general, good information content can be archieved up to about 60 or 65 km.

Since one purpose of this work was to provide a methodology to retrieve ozone at altitudes as high as possible through the backscatter technique, thirteen discrete wavelengths near the maximum of the ozone absorption cross sections below 255 nm have been chosen for the inversion.

In general, the retrieval provides fairly reliable ozone profiles within 10 % accuracy up to 50 or 55 km. Above this altitudes, the observations overestimate the true ozone content by up to 30 % at the highest altitudes of sensitivity. This is most likely reasoned by the worser tangent height retrieval with increasing altitude whose induced errors are characterized by increasing differences with altitude. Stray light was found to contami-

ACPD
7, 12097–12143, 2007

nate the limb radiances above 60 km to a remarkable extent up to 100 % relative to the ambient radiation at 75 km, but this error source was also identified to have no impact on the profile retrieval in the altitude range of interest.

Retrieval errors are also caused by inaccuracies of the solar zenith angle specification, although to a smaller extent and only at measurements at large solar zenith angles.

Comparisons with profiles from MIPAS on Envisat, HALOE, a ground based radiometer in Norway, and MLS on board AURA are mainly within the expected errors as found through sensitivity studies. The comparisons show agreement within 10 % in the upper stratosphere, and indicate an overestimation in the lower mesosphere. HALOE profiles have been modeled to the solar zenith angle condition of the collocated SCIAMACHY measurements. Comparisons of measurements in the tropics are more clearly affected by the tangent height errors than at those in the polar regions.

In summary, the methodology applied to the SCIAMACHY instrument provides reliable ozone profiles in the upper stratosphere, but reaches its limits in the mesosphere. The improvement of the tangent height misregistration will play a key role for a better ozone product from the SCIAMACHY limb scatter measurements. For the most of the scientific questions in the aimed altitude range, the retrieved ozone profiles will be accurate enough, e.g., to investigate the morphology of ozone with respect to solar cycles or atmospheric events like during solar storms if the overestimation above 50 or 55 km is considered.

If the tangent height pointing retrieval can be improved, the next step to a ozone profile product covering the troposphere to the mesosphere using Hartley and Huggins wavelengths will be made successfully. This presented work may help to minimize the error sources for this future profile retrieval.

Acknowledgements. This work was in part supported by the German Ministry of Education and Research BMBF (grant 07UFE12/8), the German Aerospace Center DLR (grant 50EE0027), the University of Bremen, and through grants-in-aid from the Natural Sciences and Engineering Research Council (NSERC) of Canada. We thank the European Space Agency (ESA) for

providing the SCIAMACHY data used in this study.

Furthermore, we are indebted to all members of the SCIAMACHY team whose efforts make all data analysis possible.

References

Amekudzi, L. K., Sinnhuber, B.-M., Sheode, N. V., Meyer, J., Rozanov, A., Lamsal, L. N., Bovensmann, H., and Burrows, J. P.: Retrieval of stratospheric NO_3 vertical profiles from SCIAMACHY lunar occultation measurement over the Antarctic, J. Geophys. Res., 110, D20304, doi:10.1029/2004JD005748, 2005. 12099

Aruga, T. and Heath, D. F.: Determination of vertical ozone distributions by spacecraft measurements using limb-scan technique, Appl. Opt., 21, 3047–3054, 1982. 12100

Bogumil, K., Orphal, J., Homann, T., Voigt, S., Spietz, P., Fleischmann, O. C., Vogel, A., Hartmann, M., Bovensmann, H., Frerick, J., and Burrows, J. P.: Measurements of molecular absorption spectra with the SCIAMACHY pre-flight model: Instrument characterization and reference data for atmospheric remote sensing in the 230–2390 nm region, J. Photochem. Photobiol. A, 157, 167–184, 2003. 12100

Bovensmann, H., Burrows, J. P., Frerick, J., Noël, S., Rozanov, V. V., Chance, K. V., and Goede, A. P. H.: SCIAMACHY: Mission objectives and measurements modes, J. Atmos. Sci., 56, 127–148, 1999. 12099

Bracher, A., Bovensmann, H., Bramstedt, K., Burrows, J. P., von Clarmann, T., Eichmann, K.-U., Fischer, H., Funke, B., Gil-López, S., Glatthor, N., Grabowski, U., Höpfner, M., Kaufmann, M., Kellmann, S., Kiefer, M., Koukouli, M. E., Linden, A., López-Puertas, M., Tsidu, G. M., Milz, M., Noël, S., Rohen, G., Rozanov, A., Rozanov, V. V., v. Savigny, C., Sinnhuber, M., Skupin, J., Steck, T., Stiller, G. P., Wang, D.-Y., Weber, M., and Wuttke, M. W.: Cross comparisons of O_3 and NO_2 measured by the atmospheric Envisat instruments GOMOS, MIPAS, and SCIAMACHY, Adv. Space Res., 36, 855–867, doi:10.1016/j.asr.2005.04.005, 2005. 12109

Brühl, C., Drayson, S. R., Russell, J. M., Crutzen, P. J., McInerney, J. M., Purcell, P. N., Claude, H., Gernandt, H., McGee, T. J., McDermid, I. S., and Gunson, M. R.: Halogen occultation experiment ozone channel validation, J. Geophys. Res., 101, 10 217–10 240, doi:10.1029/95JD02031, 1996. 12111

Buchwitz, M., de Beek, R., Noël, S., Burrows, J. P., Bovensmann, H., Bremer, H., Bergamaschi,

P., Körner, S., and Heimann, M.: Carbon monoxide, methane and carbon dioxide columns retrieved from SCIAMACHY by WMF-DOAS: Year 2003 initial data set, Atmos. Chem. Phys., 5, 3313–3329, 2005, http://www.atmos-chem-phys.net/5/3313/2005/. 12099

Burrows, J. P., Richter, A., Dehn, A., Deters, B., Himmelmann, S., Voigt, S., and Orphal, J.: Atmospheric remote-sensing reference data from GOME: 2. Temperature-dependent absorption cross sections of O_3 in the 231–794 nm range, J. Quant. Spectrosc. Radiat. Transfer, 61, 509–517, 1999. 12100, 12103, 12108

Carbary, J. F., Morrison, D., Romick, G. J., and Yee, J.-H.: Leonid meteor spectrum from 110 to 860 nm, Icarus, 161, 223–234, 2003. 12101, 12125

Chipperfield, M. P.: Multiannual simulations with a three dimensional chemical transport model, J. Geophys. Res., 104, 1781–1805, 1999. 12111

Clemesha, B. R.: Sporadic neutral metal layers in the mesosphere and lower thermosphere, J. Atmos. Sol.-Terr. Phys., 57, 725–736, 1995. 12101

Cunnold, D. M., Gray, C. R., and Merrit, D. C.: Stratospheric aerosol layer detection, J. Geophys. Res., 78, 920–931, 1973. 12100

Fleig, A., McPeters, R., Barthia, P. K., Schlesinger, B., Cebula, R., Klenk, K., Taylor, S., and Heath, D.: NIMBUS 7 Solar Backscatter Ultraviolet (SBUV) ozone products user's guide, Tech. Rep. 1234, NASA Reference Publication, 1990. 12102

Flittner, D. E., Bhartia, P. K., and Herman, B. M.: O_3 profiles retrieved from limb scatter measurements: Theory, Geophys. Res. Lett., 27, 2601–2604, 2000. 12098, 12100

Fricke, K. H., Müller, K. P., Langer, M., Römke, K., and Lübken, F. J.: Visual and lidar observations of rocket induced effects in the upper atmosphere above Andøya on 25 January 1995, in: Proc. 12th ESA Symp. on European Rocket and Balloon Programmes and Related Research, ESA-SP 370, pp. 107–112, European Space Agency, 1995. 12106

Fritzenwallner, J. and Kopp, E.: Model calculations of the silicon and magnesium chemistry in the mesosphere and lower thermosphere, Adv. Space Res., 21, 859–862, 1998. 12101

Froidevaux, L., Livesey, N. J., Reid, W. G., Jiang, Y. B., Jimenez, C., Filipiak, M. J., Schwartz, M. J., Santee, M. L., Purnphrey, H. C., Jiang, J. H., Wu, D. L., Manney, G. L., Drouin, B. J., Waters, J. W., Fetzer, E. J., Bernath, P. F., Boone, C. D., Walker, K. A., Jucks, K. W., Toon, G. C., Margitan, J. J., Sen, B., Webster, C. R., Christensen, L. E., Elkins, J. W., Atlas, E., Lueb, R. A., and Hendershot, R.: Early Validation Analysis of Atmospheric Profiles from EOS MLS on the Aura Satellite, IEEE Trans. Geosc. Rem. Sens., 44, 1106–1121, 2006. 12112

Gadsden, M. and Schröder, W.: Noctilucent clouds, Springer, New York, 1989. 12106

Glatthor, N., von Clarmann, T., Fischer, H., Funke, B., Grabowski, U., Höpfner, M., Kellmann, S., Kiefer, M., Linden, A., Milz, M., Steck, T., Stiller, G. P., Mengistu Tsidu, G., and Wang, D. Y.: Mixing processes during the Antarctic vortex split in September/October 2002 as inferred from source gas and ozone distributions from Envisat-MIPAS, J. Atmos. Sci., 62, 787–800, 2005. 12109

Glatthor, N., von Clarmann, T., Fischer, H., Funke, B., Gil-López, S., Grabowski, U., Höpfner, M., Kellmann, S., Linden, A., López-Puertas, M., Mengistu Tsidu, G., Milz, M., Steck, T., Stiller, G. P., and Wang, D.-Y.: Retrieval of stratospheric ozone profiles from MIPAS/Envisat limb emission spectra: a sensitivity study, Atmos. Chem. Phys., 6, 2767–2781, 2006, http://www.atmos-chem-phys.net/6/2767/2006/. 12109

Herzberg, G.: Spectra of Diatomic Molecules, D. van Nostrand Co., New York, 1950. 12101

Hunten, D. M., Turco, R. P., and Toon, O. B.: Smoke and dust particles of meteoric origin in the mesosphere and stratosphere, J. Atmos. Sci., 37, 1342–1357, 1980. 12106

Janz, S. J., Hilsenrath, E., Flittner, D., and Heath, D.: Rayleigh scattering attitude sensor, Proc. of SPIE, 2831, 146–153, 1996. 12104

Kaiser, J. and Burrows, J. P.: Fast weighting functions for retrievals from limb scattering measurements, J. Quant. Spectrosc. Radiat. Transfer, 77, 273–283, 2003. 12103

Kaiser, J. W., von Savigny, C., Eichmann, K.-U., Noël, S., Bovensmann, H., and Burrows, J. P.: Satellite-pointing retrieval from atmospheric limb-scattering of solar UV-B radiation, Can. J. Phys., 82, 1041–1052, 2004. 12104

Kokhanovsky, A.: Microphysical and optical properties of noctilucent clouds, Earth Sci. Rev., 71, 127–146, 2005. 12106

Langer, J.: Comparison of ozone-measurements at Ny Ålesund, Spitsbergen, in 1997 and 1998, Ph.D. thesis, University of Bremen, in German, 1999. 12112

Li, D. and Shine, K. P.: A 4-dimensional climatology of ozone for UGAMP models, UGAMP internal report 35, British Geological Survey, Department of Meteorology, University of Reading, 1995. 12102

Livesey, N. J., Read, W. G., Filipiak, M. J., Froidevaux, L., Harwood, R. S., Jiang, J. H., Jimenez, C., Pickett, H. M., Pumphrey, H. C., Santee, M. L., Schwartz, M. J., Waters, J. W., and Wu, D. L.: Earth Observing System (EOS) Microwave Limb Sounder (MLS) Version 1.5 Level 2 data quality and description document, Tech. Rep. JPL D-32381, Jet Propulsion Laboratory, California Institute of Technology, Pasadena, California, 2005. 12113

Llewellyn, E. J. and Gattinger, R. L.: Estimated OSIRIS ultraviolet/visible baffle on-orbit perfor-

mance, Tech. rep., University of Saskatchewan, 1998. 12105
Llewellyn, E. J., Lloyd, N. D., Degenstein, D. A., Gattinger, R. L., Petelina, S. V., Bourassa, A. E., Wiensz, J. T., Ivanov, E. V., McDade, I. C., Solheim, B. H., McConnell, J. C., Haley, C. S., von Savigny, C., Sioris, C. E., McLinden, C. A., Evans, W. F. J., Puckrin, E., Strong, K., Wehrle, V., Hum, R. H., Kendall, D. J. W., Matsushita, J., Murtagh, D. P., Brohede, S., Stegman, J., Witt, G., Barnes, G., Payne, W. F., Piché, L., Smith, K., Warshaw, G., Deslauniers, D.-L., Marchand, P., Richardson, E. H., King, R. A., Wever, I., McCreath, W., Kyrölä, E., Oikarinen, L., Leppelmeier, G. W., Auvinen, H., Mégie, G., Hauchcorne, A., Lefévre, F., de la Nöe, J., Ricaud, P., Frisk, U., Sjoberg, F., von Schéele, F., and Nordh, L.: The OSIRIS instrument on the Odin spacecraft, Can. J. Phys., 82, 411–422, 2004. 12105
López-Puertas, M.: Definition of observational requirements for support to a future Earth explorer atmospheric chemistry mission, Tech. Rep. ESTEC Contract Number 13048/98/NL/DG, WP 6000: Molecular Non-Local Thermodynamic Equilibrium Working Document V2.0, Instituto de Astrofísica de Andalucía (CSIC), Granada, Spain, 2000. 12101, 12124
Loughman, R. P., Flittner, D. E., Herman, B. M., Bhartia, P. K., Hilsenrath, E., and McPeters, R. D.: Description and sensitivity analysis of a limb scattering ozone retrieval algorithm, J. Geophys. Res., 110, D19 301, doi:10.129/2004JD005429, 2005. 12106
Lumpe, J. D., Randall, C. E., Bevilacqua, R. M., Hoppel, K. W., Nedoluha, G. E., and Prados, A. I.: POAM III Validation Summary, AGU Fall Meeting Abstracts, p. D711, 2003. 12109
McCormick, M. P., Zawodny, J. P., Larsen, J. C., and Wang, P. H.: An overview of SAGE I and II ozone measurements, Planet. Space Sci., 37, 1567–1586, 1989. 12102
McLinden, C. A., Olsen, S. C., Hannegan, B., Wild, O., and Prather, M. J.: Stratospheric ozone in 3-D models: A simple chemistry and the cross-tropopause flux, J. Geophys. Res., 105, 14 653–14 665, 2000. 12103
McPeters, R.: Ozone profile comparisons, in: The Atmospheric Effects of Stratospheric Aircraft: Report of the 1992 Models and Measurement Workshop, no. 1292 in NASA Reference Publ., pp. D31–D37, M. J. Prather and E. E. Remsberg, 1993. 12103
McPeters, R. D., Janz, S. J., Hilsenrath, E., Brown, T. L., Flittner, D. E., and Heath, D. F.: The retrieval of O_3 profiles from limb scatter measurements: Results from the Shuttle Ozone Limb Sounding Experiment, Geophys. Res. Lett., 27, 2597–2600, 2000. 12098, 12100, 12101, 12104
Meyer, J., Bracher, A., Rozanov, A., Schlesier, A. C., Bovensmann, H., and Burrows, J. P.: Solar

occultation with SCIAMACHY: algorithm description and first validation, Atmos. Chem. Phys., 5, 1589–1604, 2005, http://www.atmos-chem-phys.net/5/1589/2005/. 12099
Nagatani, R. M. and Rosenfield, J. E.: Temperature, net heating and circulation, in: The Effect of Stratospheric Aircraft: Report of the 1992 Models and Measurement Workshop, no. 1292 in NASA Reference Publ., pp. A1–A47, M. J. Prather and E. E. Remsberg, 1993. 12103
Natarajan, M. L., Deaver, L. E., Thompson, E., and Magill, B.: Impact of twilight gradients on the retrieval of mesospheric ozone from HALOE, J. Geophys. Res., 110, 2005. 12111
Nazarayan, H., McCormick, M. P., and Russell, J. M.: New studies of SAGE II and HALOE ozone profile and long-term change comparisons, J. Geophys. Res. (Atmos.), 110, 9305, 2005. 12111
Oikarinen, L., Sivhola, E., and Kyrölä, E.: Multiple-scattering radiance in limb-viewing geometry, J. Geophys. Res., 104, 31 261–31 274, 1999. 12106
Palm, M., von Savigny, C., Warneke, T., Velazco, V., Notholt, J., Künzi, K., Burrows, J., and Schrems, O.: Intercomparison of O_3 profiles observed by SCIAMACHY and ground based microwave instruments, Atmos. Chem. Phys., 5, 2091–2098, 2005, http://www.atmos-chem-phys.net/5/2091/2005/. 12112
Rees, M. H.: Physics and chemistry of the upper atmosphere, Cambridge University Press, Cambridge, 1989. 12101
Rodgers, C. D.: Retrieval of atmospheric temperature and composition from remote measurements of thermal radiation, Rev. Geophys. Space Phys., 14, 609–624, 1976. 12102, 12103
Rohen, G., von Savigny, C., Sinnhuber, M., Llewellyn, E. J., Kaiser, J. W., Jackman, C. H., Kallenrode, M.-B., Schröter, J., Eichmann, K.-U., Bovensmann, H., and Burrows, J. P.: Ozone depletion during the solar proton events of October/November 2003 as seen by SCIAMACHY, J. Geophys. Res., 110, A09S39, doi:10.1029/2004JA010984, 2005. 12098, 12104, 12109
Rohen, G. J.: Retrieval of Upper Stratospheric and Lower Mesospheric Ozone Profiles from SCIAMACHY Limb Scatter Measurements and Observations of the Ozone Depletion During the Solar Proton Event in October and November 2003, Logos Publication, Berlin, Ph.-D. thesis, ISBN 978-3-3825-1363-4, ISSN 1615-6862, 2006. 12111
Rohen, G. J., von Savigny, C., Llewellyn, E. J., Kaiser, J. W., Eichmann, K.-U., Bracher, A., Bovensmann, H., and Burrows, J. P.: First results of ozone profiles between 35 and 65 km retrieved from SCIAMACHY limb spectra and observations of ozone depletion during the solar proton events in Oct./Nov. 2003, Adv. Space Res., 37, 2263–2268, doi:10.1016/j.asr.200503.160, 2006. 12107

Rozanov, A., Bovensmann, H., Bracher, A., Hrechanyy, S., Rozanov, V., Sinnhuber, M., Stroh, F., and Burrows, J. P.: NO_2 and BrO vertical profile retrieval from SCIAMACHY limb measurements: Sensitivity studies, Adv. Space Res., 36, 846–854, 2005. 12100

Rusch, D. W., Mount, G. H., Barth, C. A., Rottmann, G. J., Thomas, R. J., Thomas, G. E., Sanders, R. W., Lawrence, G. M., and Eckman, R. S.: Ozone densities in the lower mesosphere measured by a limb scanning UltraViolet Spectrometer, Geophys. Res. Lett., 10, 241–244, 1983. 12098, 12100

Rusch, D. W., Bevilacqua, R. M., Randall, C. E., Lumpe, J. D., Hoppel, K. W., Fromm, M. D., Debrestian, D. J., Olivero, J. J., Hornstein, J. H., Guo, F., and Shettle, E. P.: Validation of POAM ozone measurements with coincident MLS, HALOE, and SAGE II observations, J. Geophys. Res., 102, 23 615–23 628, 1997. 12111

Russell, J. M., Gordley, L. L., Park, J. H., Drayson, S. R., Hesketh, W. D., Cicerone, R. J., Tuck, A. F., Frederick, J. E., Harries, J. E., and Crutzen, P. J.: The Halogen Occultation Experiment, J. Geophys. Res., 98, 10 777–10 797, 1993. 12111

Schwab, A., Mager, R., and Fricke, W.: SCIAMACHY pointing error budget, Tech. Rep. TN-SCIA-0000DO/06, A, Dornier, 1996. 12099

Sioris, C. E., Haley, C. S., McLinden, C. A., von Savigny, C., McDade, I. C., McConnell, J. C., Evans, W. F. J., Lloyd, N. D., Llewellyn, E. J., Chance, K. V., Kurosu, T. P., Murtagh, D., Frisk, U., Pfeilsticker, K., Bösch, H., Weidner, F., Strong, K., Stegman, J., and Mégie, G.: Stratospheric profiles of nitrogen dioxide observed by OSIRIS on the Odin satellite, J. Geophys. Res., 108, 4215–4234, doi:101029/2002JD002672, 2003. 12104

Steck, T., von Clarmann, T., Fischer, H., Funke, B., Glatthor, N., Grabowski, U., Höpfner, M., Kellmann, S., Kiefer, M., Linden, A., Milz, M., Stiller, G. P., Wang, D. Y., Allaart, M., Blumenstock, T., von der Gathen, P., Hansen, G., Hase, F., Hochschild, G., Kopp, G., Kyrölä, E., Oelhaf, H., Raffalski, U., Marrero, A. R., Remsberg, E., III, J. R., Stebel, K., Steinbrecht, W., Wetzel, G., Yela, M., and Zhang, G.: Bias determination and precision validation of ozone profiles from MIPAS-Envisat retrieved with the IMK-IAA processor, Atmos. Chem. Phys., 7, 4427–4480, 2007, http://www.atmos-chem-phys.net/7/4427/2007/. 12109

Thomas, G. E., Barth, C. A., Hansen, E. R., Hord, C. W., Mount, G. M., Rottman, G. H., Rusch, D. W., Stewart, A. I., Thomas, R. J., London, J., Bailey, P. L., Crutzen, P. J., Dickenson, R. E., Gille, J. C., Liu, S. C., Noxon, J. J., and Farmer, C. B.: Scientific objectives of the Solar Mesosphere Explorer mission, Pure Appl. Geophys., 118, 591–615, 1980. 12098

van Soest, G.: Investigation of SCIAMACHY limb spatial straylight, Tech. Rep. SRON-EOS-RP-

05-006, SRON, 2005. 12105
von Clarmann, T., Fischer, H., Funke, B., Glatthor, N., Grabowski, U., Höpfner, M., Kiefer, M., Martin-Torres, F. J., Milz, M., and Stiller, G. P.: MIPAS interactive semi-operational level-2 data processing, in: Current Problems in Atmospheric Radiation, edited by: Smith, W. L. and Timofeyev, Y. M., pp. 785–788, A. Deepak Publ., Hampton, Va., 2001. 12109
von Clarmann, T., Glatthor, N., Grabowski, U., Höpfner, M., Kellmann, S., Kiefer, M., Linden, A., Mengistu Tsidu, G., Milz, M., Steck, T., Stiller, G. P., Wang, D. Y., Fischer, H., Funke, B., Gil-López, S., and López-Puertas, M.: Retrieval of temperature and tangent altitude pointing from limb emission spectra recorded from space by the Michelson Interferometer for Passive Atmospheric Sounding (MIPAS), J. Geophys. Res., 108, 2003. 12104, 12109
von Savigny, C.: Retrieval of Stratospheric Ozone Density Profiles from OSIRIS Scattered Sunlight Observations, Ph.D. thesis, York University Toronto, 2002. 12105, 12107
von Savigny, C., Haley, C. S., Sioris, C. E., McDade, I. C., Llewellyn, E. J., Degenstein, D., Evans, W. F. J., Gattinger, R. L., Griffioen, E., Kyrölä, E., Lloyd, N. D., McConnell, J. C., McLinden, C. A., Mégie, G., Murtagh, D. P., Solheim, B., and Strong, K.: Stratospheric ozone profiles retrieved from limb scattered sunlight radiance spectra measured by the OSIRIS instrument on the Odin satellite, Geophys. Res. Lett., 30, 1755, 2003a. 12100
von Savigny, C., Rozanov, A., Bovensmann, H., and Kaiser, J. W.: SCIAMACHY limb pointing analysis report, Tech. rep., University of Bremen, 2003b. 12104
von Savigny, C., Kaiser, J. W., Bovensmann, H., Burrows, J. P., McDermid, I. S., and Leblanc, T.: Spatial and temporal characterization of SCIAMACHY limb pointing errors during the first three years of the mission, Atmos. Chem. Phys., 5, 2593–2602, 2005a. 12104
von Savigny, C., Rozanov, A., Bovensmann, H., Eichmann, K.-U., Noël, S., Rozanov, V., Sinnhuber, B.-M., Weber, M., Burrows, J. P., and Kaiser, J. W.: The ozone hole breakup in September 2002 as seen by SCIAMACHY on Envisat., J. Atmos. Sci., 62, 721–734, 2005b. 12107
von Savigny, C., Ulasi, E., Eichmann, K.-U., Bovensmann, H., and Burrows, J.: Detection and mapping of polar stratospheric clouds using limb scattering observations, Atmos. Chem. Phys., 5, 3071–3079, 2005c. 12106
Wayne, R. P.: The photochemistry of ozone, Atmos. Env., 21, 1683–1694, 1987. 12100

Table 1. Summary of the sensitivity studies. The errors are given in %.

Altitude [km]	35	39	45	51	57	65
Pointing errors[1]	6.0	10.5	14.5	15.5	16.5	17.0
Solar zenith angle[2]	13.0	11.0	9.5	11.5	12.8	8.5
Stray light	0.0	0.0	0.0	0.2	0.4	0.5
Omitting double scattering	2.3	0.8	0.2	0.0	0.0	0.0
Omitting albedo (A)	2.0	0.6	0.2	0.0	0.0	0.0
A-priori[3]	12.0	1.0	2.0	2.5	3.0	7.0
Background density[4]	0.7	1.2	0.7	0.2	0.1	0.1
Cross sections[5]	4.0	7.0	5.0	2.0	1.0	2.0
Sum (1σ)	21.5	16.8	18.2	19.6	21.1	20.4

[1] Δ=0.5 km
[2] Δ=2°
[3] Δ=50%
[4] Δ=5%
[5] Δ=20 K

ACPD
7, 12097–12143, 2007

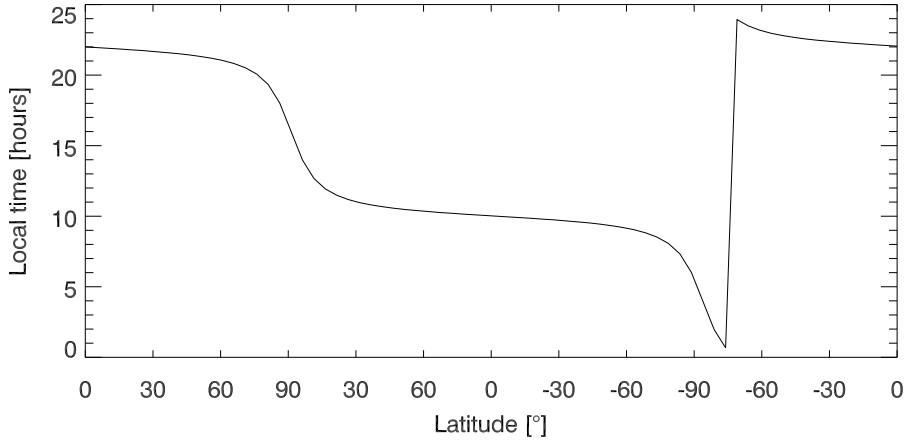

Fig. 1. Envisat's local overflight times, beginning at 0° latitude on the night side of the Earth. Although not indicated here, both Earth poles are not overflown in a regular orbit due to an inclination angle unequal 90°.

ACPD
7, 12097–12143, 2007

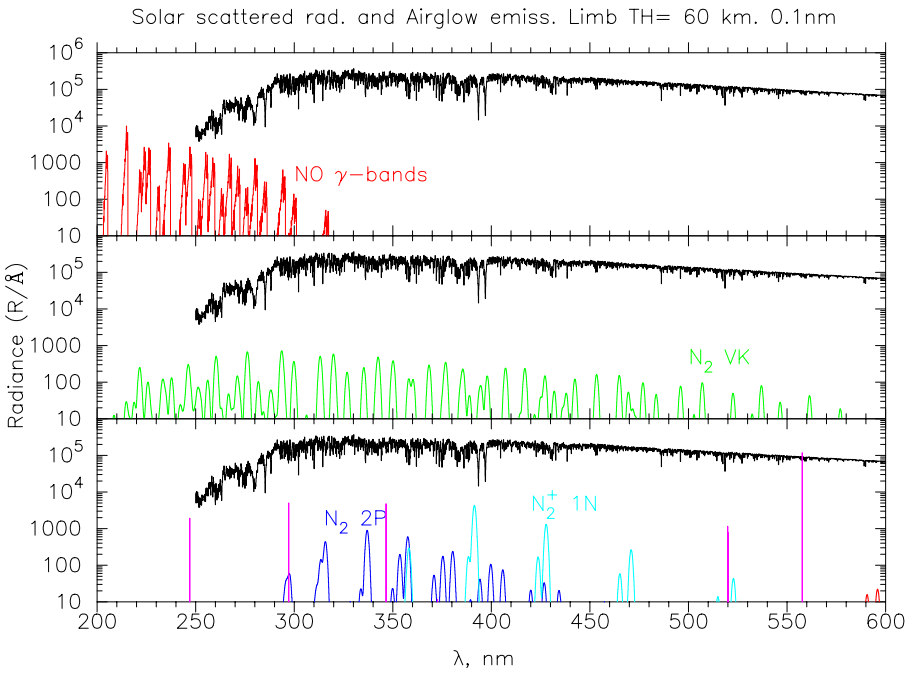

Fig. 2. Modeled airglow emissions in limb viewing mode in the ultraviolet at 60 km tangent height (colored), spectral resolution 0.1 nm. Also depicted are the modeled total limb radiances (black). At lower wavelengths, the intensity of modeled emissions reaches the ambient limb radiances. Remarkable is the intensity of the atmomic oxygen green line at 577.7 nm. Figure taken from López-Puertas (2000).

ACPD
7, 12097–12143, 2007

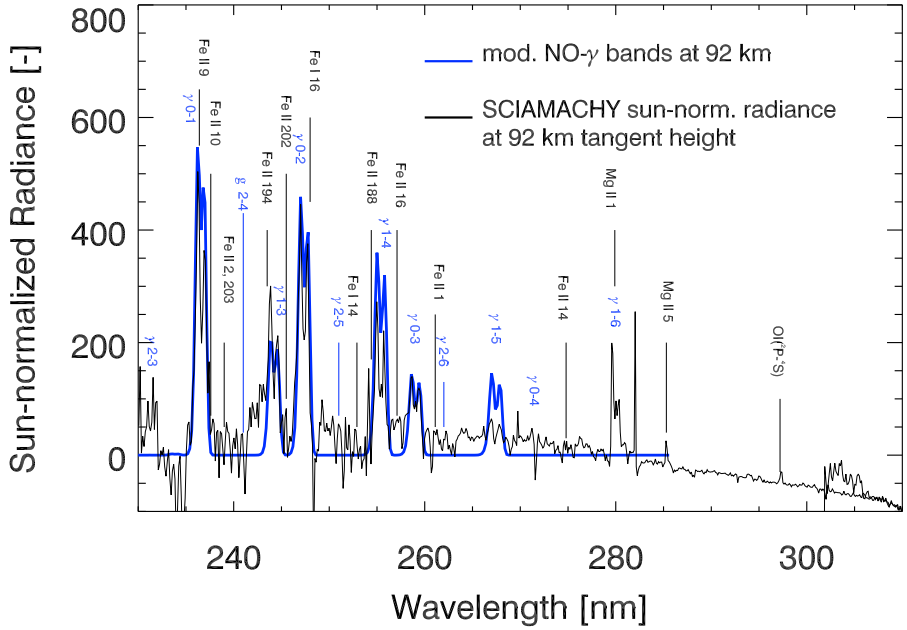

Fig. 3. Averaged sun-normalized limb spectrum from 430 SCIAMACHY limb radiance measurements on arbitrary chosen days in spring 2004 at 92 km tangent height. A NO-γ emission model at 213 K is over-plotted. Vibrational NO-γ transitions are denoted, as well as expected metal emissions from a LEONID spectrum (Carbary et al., 2003). The second black line above 300 nm indicates the beginning of the second SCIAMACHY spectral channel.

ACPD
7, 12097–12143, 2007

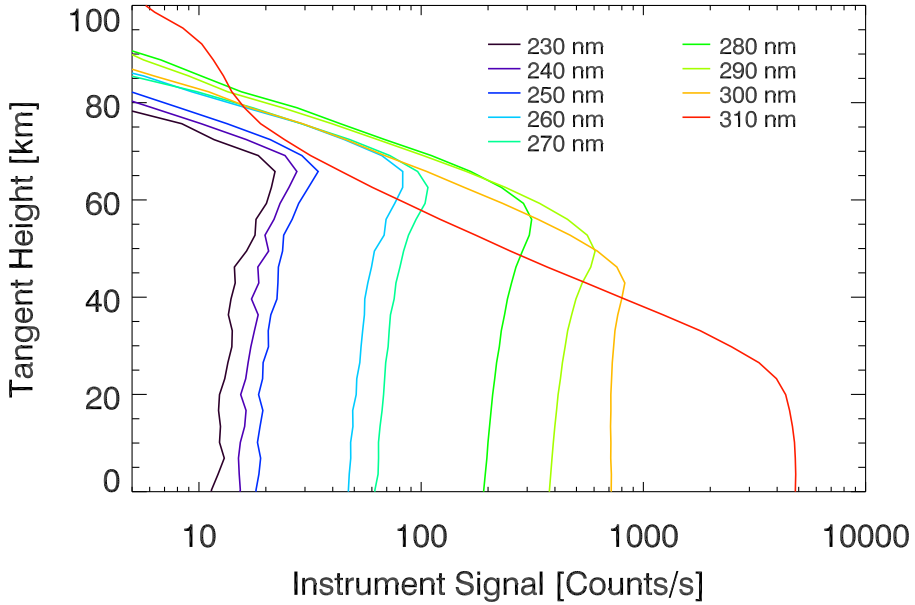

Fig. 4. Example of SCIAMACHY limb radiance profiles between 230 and 310 nm. The feature at the 310 nm radiance profile above 70 km is caused by stray light and will be discussed later in the section about the sensitivity studies.

ACPD
7, 12097–12143, 2007

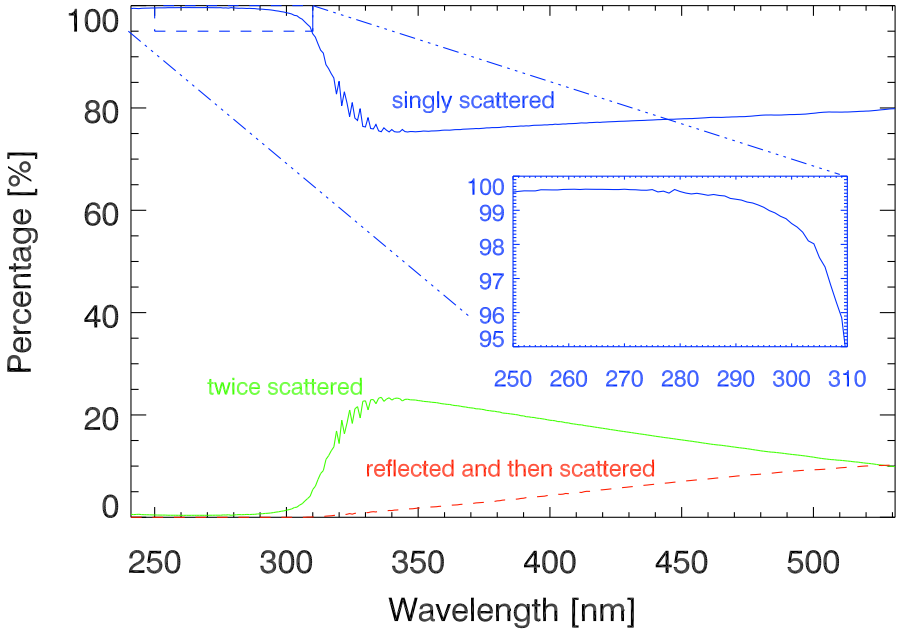

Fig. 5. Fraction of scattered and reflected photons at 60 km tangent height as modeled by SCIARAYS. Ozone absorption is considered, albedo=0.5. Similar model runs have shown that the fraction of double scattering at 30 km altitude is only slightly enlarged by a few percent.

ACPD
7, 12097–12143, 2007

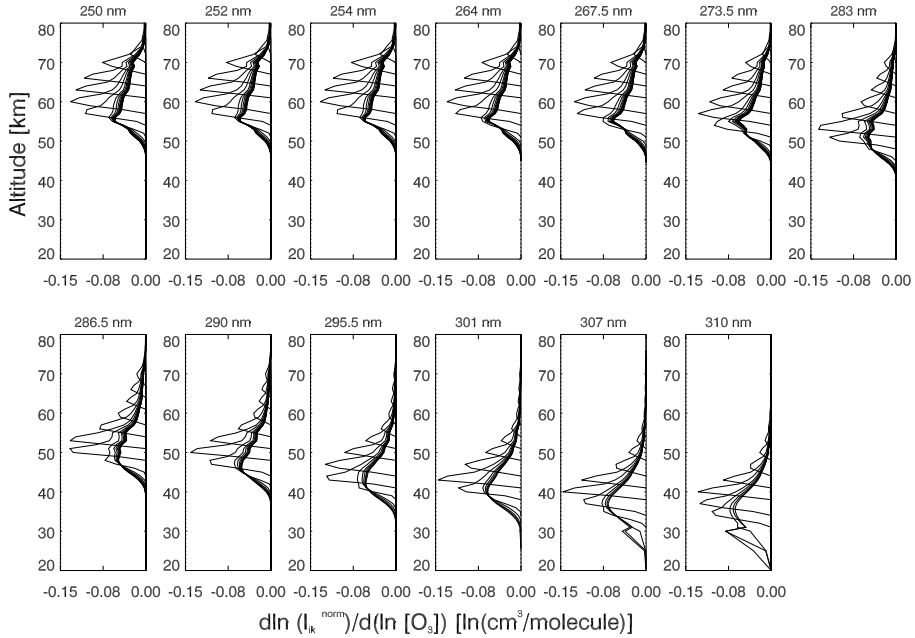

Fig. 6. Weighting functions for all thirteen wavelengths and all tangent heights from a sample profile retrieval. Solar zenith angle is 79°.

ACPD
7, 12097–12143, 2007

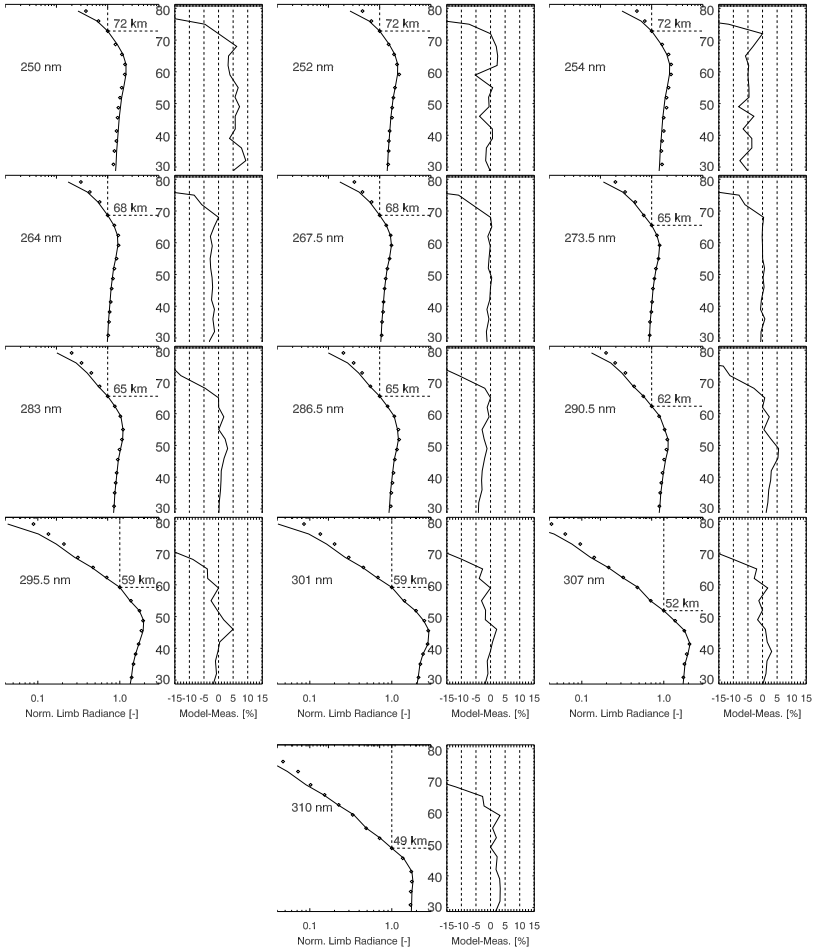

Fig. 7.

ACPD
7, 12097–12143, 2007

Fig. 7. Fits of limb radiance profiles for all thirteen wavelengths (sample profile retrieval, orbit 10945, number 1521, state 3). Dots in the respective left panels denote the measurement, the solid lines the model. Radiance profiles are normalized at a certain altitude, respectively. Residuals are depicted in the right panel of the figures. Above 70 km, the measurements are underestimated by the model due to stray light contaminations.

ACPD

7, 12097–12143, 2007

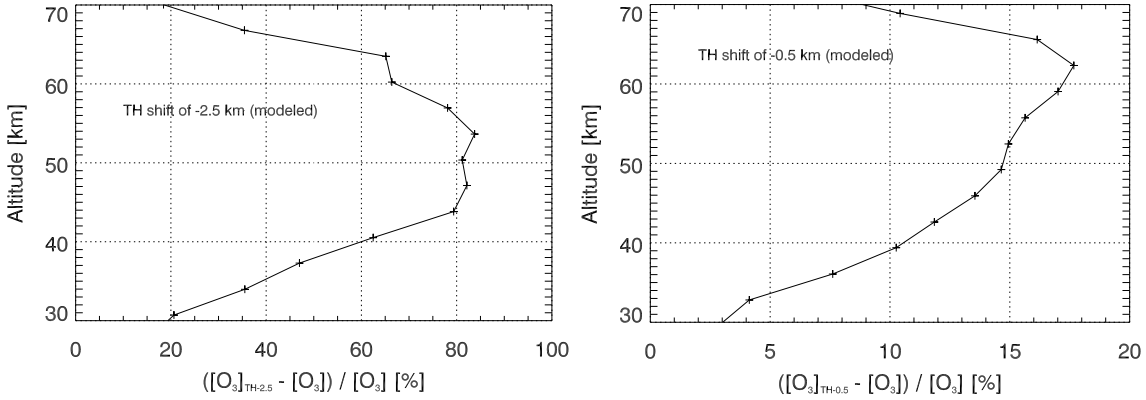

Fig. 8. Errors of sample profile induced by virtual tangent height shifts of –2.5 km (left) and –0.5 km (right).

ACPD
7, 12097–12143, 2007

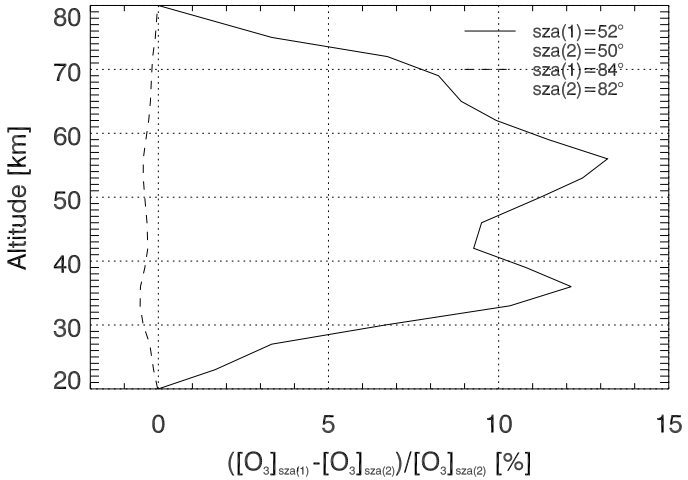

Fig. 9. Retrieval errors caused by an inacurracy in the solar zenith angle of 2° at 82 and 50° ((orbit 05387, number 1244, state 9) and (orbit 05387, number 1244, state 4)).

ACPD
7, 12097–12143, 2007

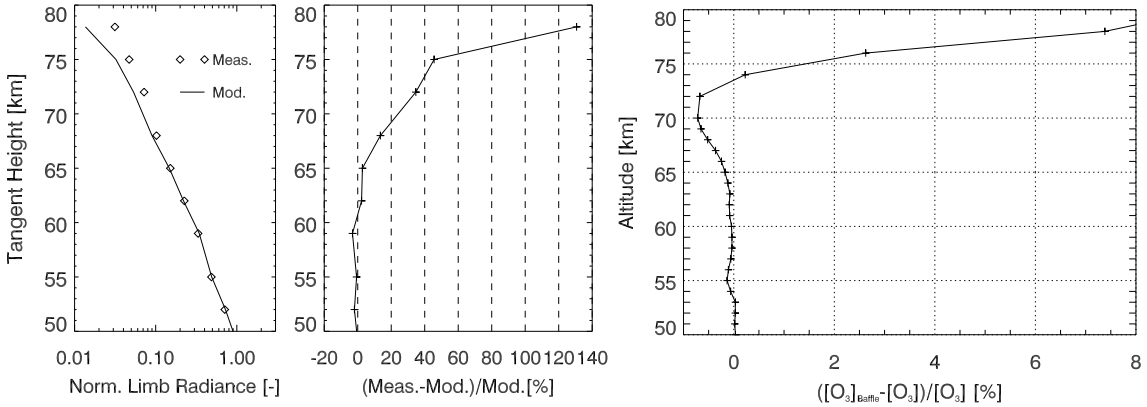

Fig. 10. Left: Simulated and measured limb radiances at 310 nm from a sample retrieval and their difference in percent, indicating the contribution of stray light contamination. The right figure shows the stray light induced errors on the retrieval in percent.

ACPD
7, 12097–12143, 2007

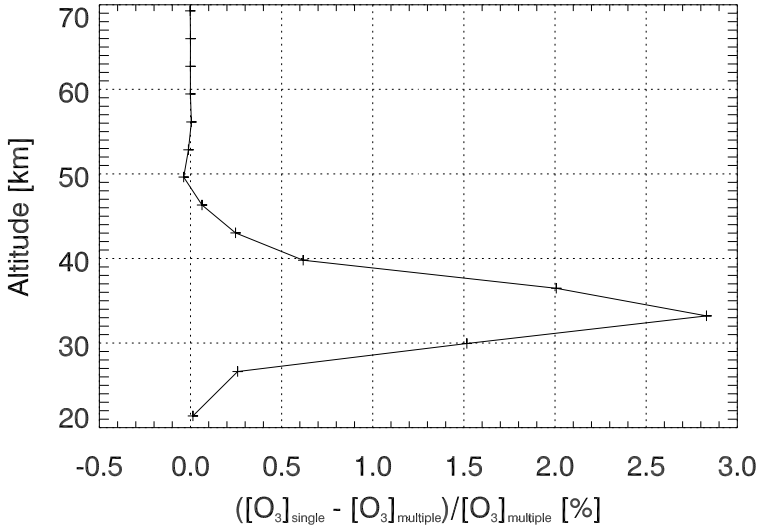

Fig. 11. Retrieval errors induced by omitting double scattering (sample inversion, solar zenith angle 35°).

ACPD
7, 12097–12143, 2007

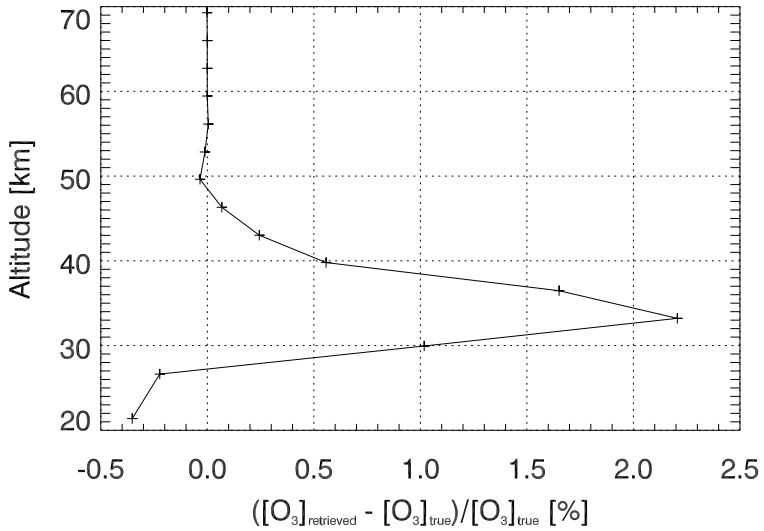

Fig. 12. Maximal errors induced by omitting aerosols, 35° solar zenith angle.

ACPD
7, 12097–12143, 2007

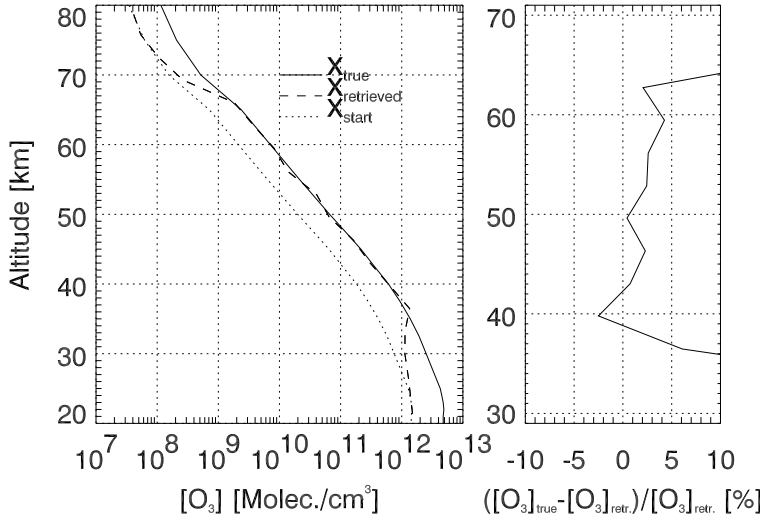

Fig. 13. Errors induced by different a priori profiles which differ by 50 %. x_{start} denotes the a priori profile.

ACPD
7, 12097–12143, 2007

EGU

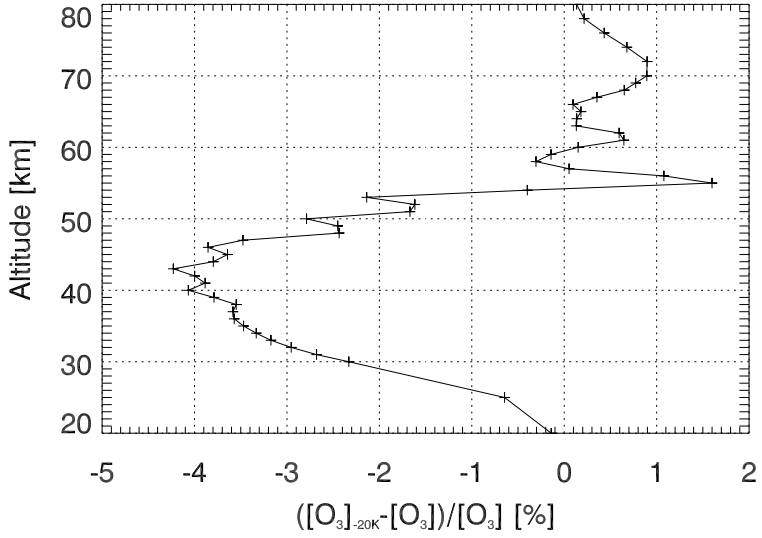

Fig. 14. Errors of a sample profile using absorption cross sections at a 20° higher temperature (273 and 293 K).

ACPD
7, 12097–12143, 2007

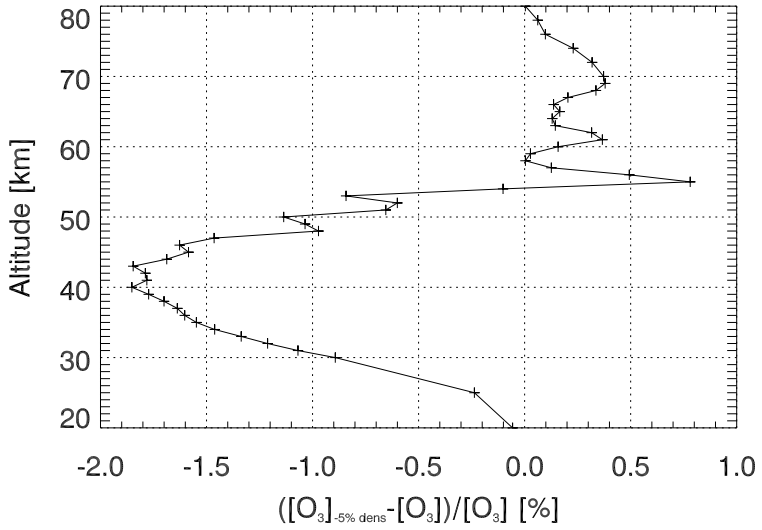

Fig. 15. Errors induced by lowering the air density by 5 %.

ACPD
7, 12097–12143, 2007

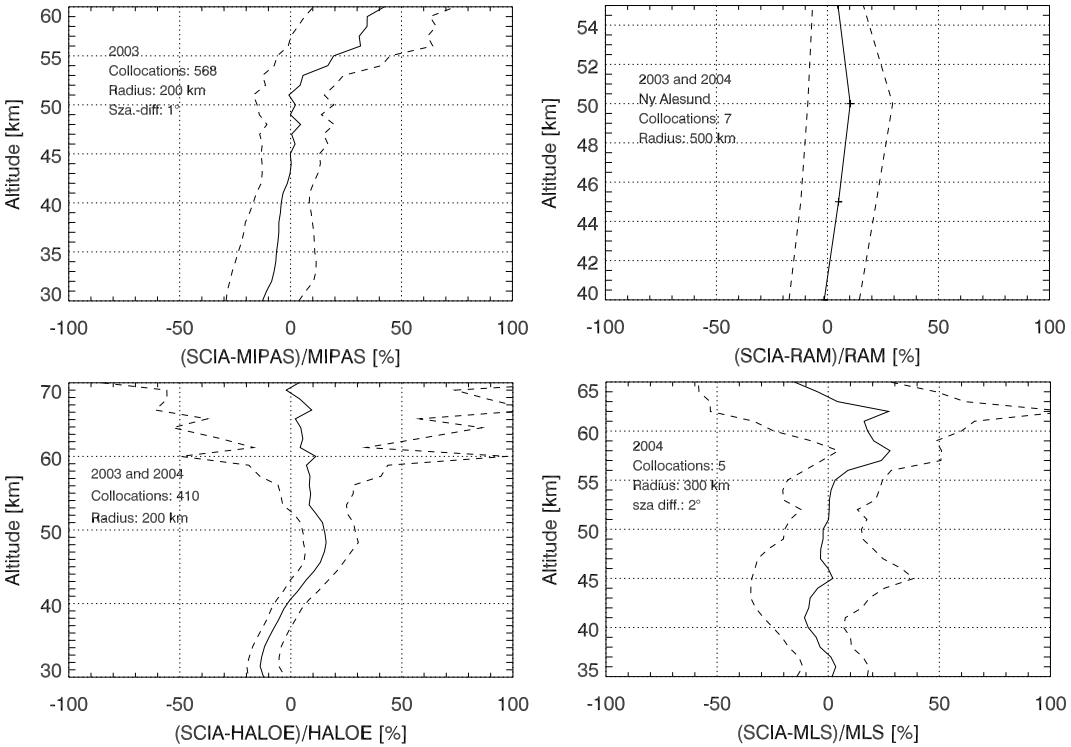

Fig. 16. Statistics from comparisons with profiles from MIPAS, RAM, HALOE, and MLS. Solid lines denote the mean deviation and dashed lines the 1σ standard deviation.

ACPD
7, 12097–12143, 2007

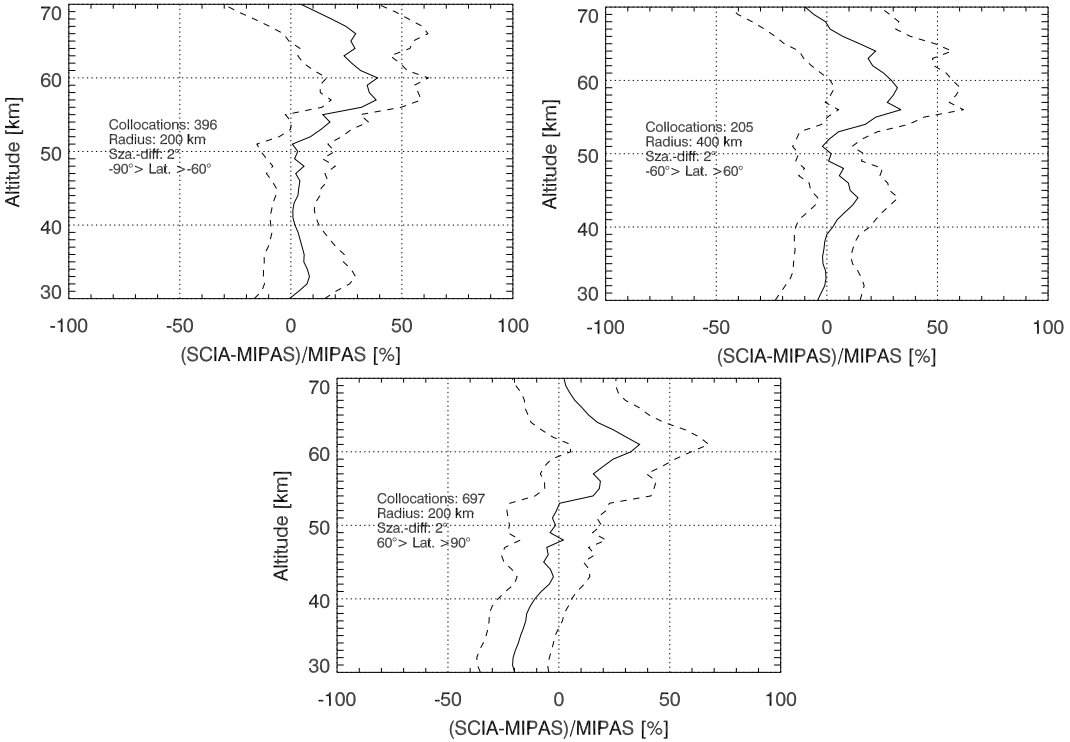

Fig. 17. Statistics of averaged comparisons in 2003 and 2004 with MIPAS profiles for three latitude bands.

ACPD
7, 12097–12143, 2007

EGU

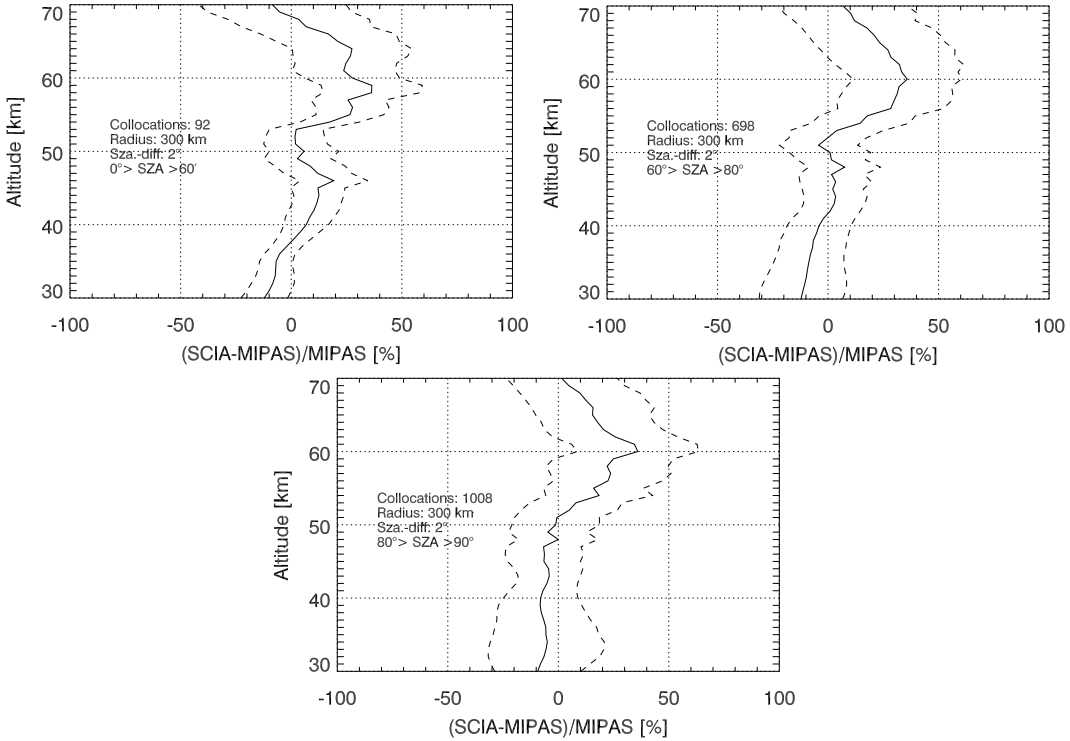

Fig. 18. Comparison with MIPAS profiles in 2003 and 2004 at different solar zenith angle ranges.

ACPD
7, 12097–12143, 2007

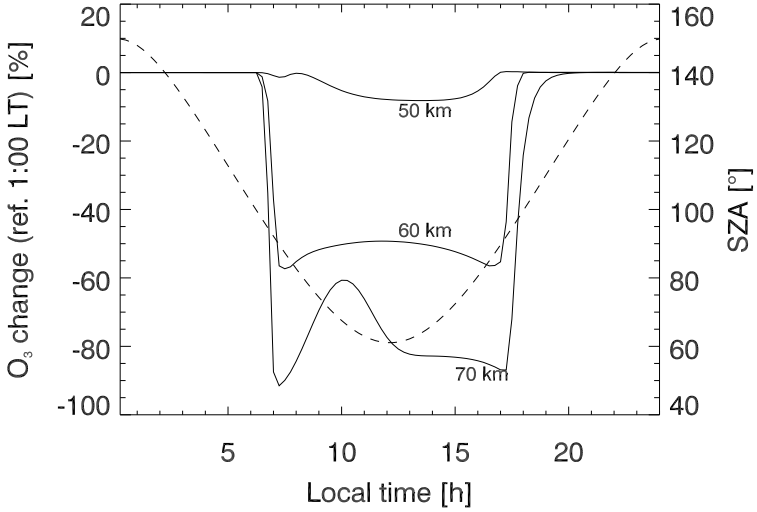

Fig. 19. SLIMCAT simulation of diurnal variability of ozone at 50, 60 and 70 km on 11 August 2002. The dashed line denotes the solar zenith angle and the solid lines denote the ozone changes at the respective altitudes.

ACPD
7, 12097–12143, 2007

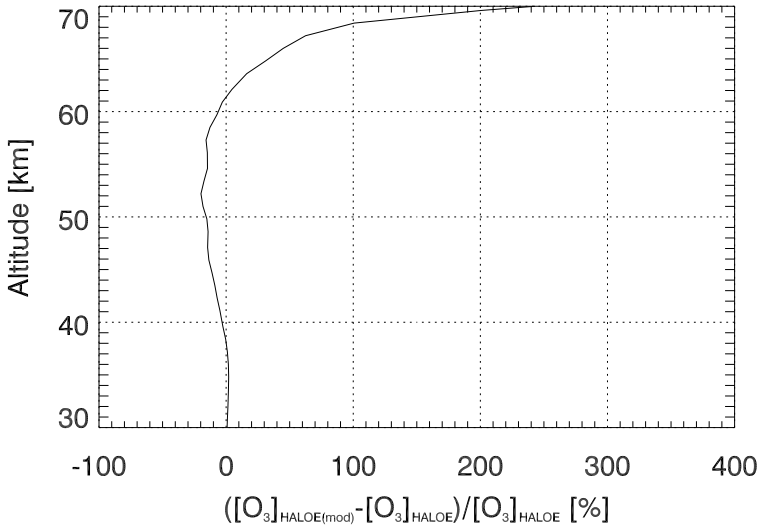

Fig. 20. Relative differences between a HALOE sample ozone profile – photochemically modeled to 74° – and HALOE profile at 90° solar zenith angle.

ACPD
7, 12097–12143, 2007